3D Coronary MRA Integrated in a Fast and Comprehensive Free-breathing CMR Exam

Juliano Lara Fernandes, M.D., Ph.D., M.B.A.[1]; Karl P. Kunze, Ph.D.[2]; Claudia Prieto, Ph.D.[3]; Rene Botnar, Ph.D.[3]

[1]Cardiovascular Department, Radiologia Clinica de Campinas, Jose Michel Kalaf Research Institute, Campinas, SP, Brazil
[2]MR Research Collaborations, Siemens Healthineers, Frimley, UK
[3]Department of Biomedical Engineering, King's College London, UK

Introduction

Coronary artery disease (CAD) evaluation is one of the cornerstones of cardiovascular imaging. Cardiovascular magnetic resonance (CMR) has been shown to have many advantages in the assessment of the disease, and multiple randomized multi-center trials have demonstrated its diagnostic and prognostic capabilities [1–4]. The evaluation of CAD by CMR has mostly focused on identifying relevant functional information regarding myocardial perfusion, and associating that evidence with left ventricular global and regional function, as well as with scar data from late gadolinium enhancement (LGE) images. Most studies have used qualitative assessment of myocardial perfusion as an indication of significant coronary stenosis, but more recently automated quantitative stress perfusion has been made available for routine clinical workflows [5].

Despite the important functional information provided by CMR, the increased availability of, and clinical results from studies using coronary computed tomography angiography (CCTA), as well as recent findings in the ISCHEMIA trials, have raised questions about whether an anatomical or functional test is better for assessing CAD [6,7]. While a more thorough discussion of the debate is beyond the scope of this manuscript, recent ESC guidelines for stable CAD have been revised to incorporate anatomical evaluation as a first-line diagnostic test, especially in patients with a low-to-intermediate likelihood of obstructive disease [8].

The role for CMR in the assessment of CAD in this ever-changing environment will require further critical developments given these recent clinical findings. On

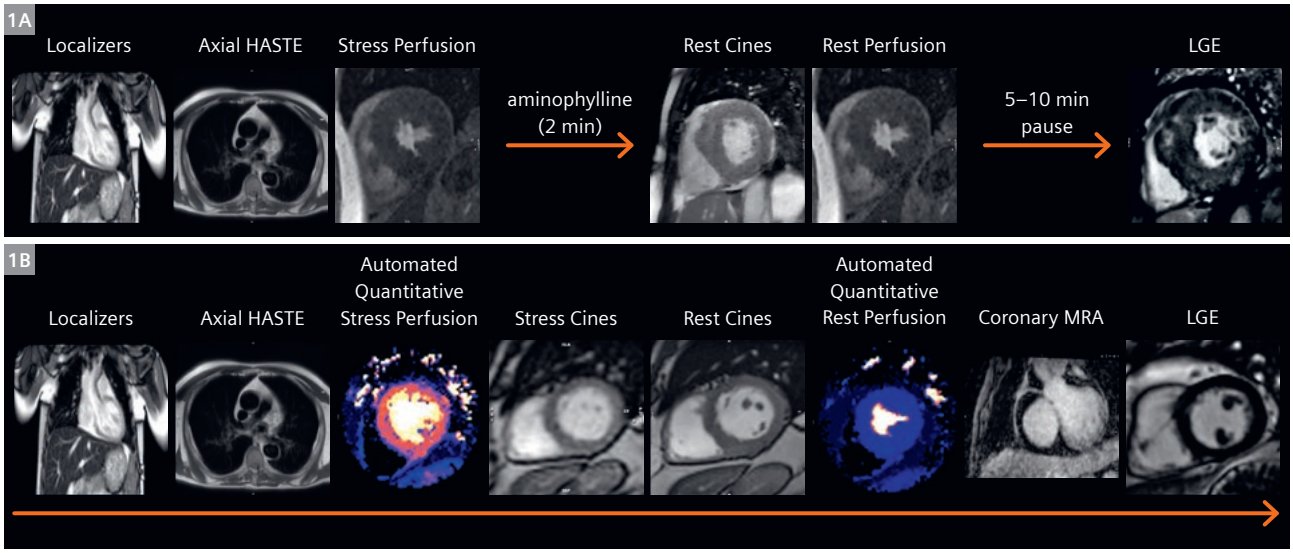

1 **(1A)** The first routine free-breathing (FB) protocol used in 2017, which did not incorporate quantitative perfusion data or coronary magnetic resonance angiography (MRA); **(1B)** the latest version of the protocol with the quantitative perfusion data, plus the stress cine images and coronary MRA included in the temporal gaps of the first protocol, with limited time penalty. The whole stress protocol takes around 30 minutes to complete.

the one hand, we have a technique that has many unique features, robust clinical evidence of effectiveness, and an advantageous cost-effectiveness ratio in CAD evaluation [9]. On the other hand, the modality remains under-utilized in most parts of the world [10], is still considered a time-consuming imaging exam, and so far offers limited evidence for providing routine clinical assessment of coronary anatomy. 3D coronary magnetic resonance angiography (CMRA) has been available for more than two decades [11], but limited spatial resolution and heart coverage, long unpredictable (due to respiratory gating), and associated image degradation due to respiratory motion acquisition times have prevented its more widespread use [12]. Recent technical developments in free-breathing whole-heart CMRA including the use of artificial intelligence (AI), faster acquisition sequences, and motion-compensated reconstruction have made it possible to provide images that are clinically useful within a clinical environment [13]. Integrating the newer anatomical data provided by these sequences to the already established functional CMR exam is still a challenge. In the following, we try to provide a framework which we believe can help CMR to overcome some of the hurdles involved in this integration and offer a truly comprehensive approach to provide both anatomical and quantitative functional data for CAD in a relatively short time slot while still maintaining its cost-effectiveness.

A complete free-breathing protocol

In 2017, we started using a free-breathing (FB) protocol routinely in our clinical scans with a MAGNETOM Verio 3T scanner [14], which we later upgraded to a MAGNETOM Skyra^{fit}. The initial FB protocol is shown in Figure 1A. In summary, it contained routine orthogonal and cardiac axis localizers, an axial black-blood T1-weighted half-Fourier single-shot turbo spin echo (HASTE) sequence, a multi-slice FLASH perfusion sequence, a prototype compressed sensing cine bSSFP sequence with sparse sampling and iterative reconstruction, and a prototype respiratory motion-corrected bSSFP averaged phase-sensitive inversion recovery sequence (MOCO-PSIR-LGE) that was reconstructed in-line using the Gadgetron framework [15, 16]. Spatial and temporal resolution of the FB sequences matched clinically used breath-hold protocols. The FB protocol allowed us to perform a cardiac scan in 21.0 ± 5.1 minutes (range 14 to 27 minutes) with comparable image quality to routine breath-hold protocols.

As technology development occurred, we were able to further improve image quality and information gathered during the FB exam by incorporating new sequences that, while providing the same speed of acquisition and FB capabilities, also included new automated features using AI or faster, cloud-based post-processing. The current protocol uses a dual sequence perfusion protocol with in-line, fully automated analysis within a 2-minute reconstruction time [17]. This quantitative approach has been validated against PET perfusion and provides a comprehensive evaluation of ventricular perfusion with no additional acquisition time or manual post-processing [18]. The ability to have quantitative data without the need to change the usual single infusion workflow by using the dual sequence approach, makes this sequence very practical without the need to change any of our routine setup.

In addition to that, we are now able to acquire a full dataset of cine images during vasodilatory stress, comprising a total of 15 slices (three 4-chamber, three 2-chamber, and nine short-axis slices) in less than 1 minute while aminophylline is being administered to the patient. This sequence uses real-time cine images with non-linear reconstruction to provide rapid acquisition times with the high temporal resolution necessary for evaluating possible regional dysfunction during stress [19]. After stress reversal, we can now move on to acquire high-resolution cine images that require more computational power and use a distributed cloud-based solution within the Gadgetron framework [20]. This sequence uses a re-binning scheme from multiple real-time images, which are motion-corrected and averaged to provide a high signal-to-noise ratio as well as high temporal resolution [21]. The additional quantitative perfusion, stress cines, and binning rest cines provide a significant improvement in image quality and quantitative information without adding to the total exam time.

Coronary MRA – the missing link

Despite now having a full FB protocol that provided us with most of the functional data for CAD evaluation, the protocol still included 5 to 10 minutes of dead time after the second contrast infusion for the first-pass rest perfusion while waiting for the LGE acquisitions. In our view, this was the perfect time slot to acquire a coronary MRA that would add anatomical information to the functional information already available.

Twenty years ago, a seminal paper by Kim et al. demonstrated the first true clinical application for coronary MRA [11]. Despite never having really fulfilled its original promise, the use of coronary MRA has significantly evolved over the last few years with the development of many new technical advances that use a combination of faster imaging, more robust respiratory motion correction, and enhanced reconstruction methods to boost both spatial resolution and whole-heart coverage [13]. This has paved the way for the development of new sequences that provide isotropic < 1 mm resolution, simplified 3D scan planning, and reasonable reconstruction times, giving

coronary MRA a true shot at competing with other modalities, especially cardiac CTA [22].

The addition of coronary MRA to perfusion analysis has generated mixed results in recent years [23–25]. The lack of added value for coronary MRA stems partly from earlier technical limitations of the sequences, unpredictable scan time [26], and their particular use in intermediate- to high-risk populations where functional information seems more important. Using more recent techniques, Zhang et al. showed that contrast-enhanced coronary MRA performed at 3T significantly improved sensitivity and diagnostic accuracy versus perfusion/LGE CMR alone [27]. This is in line with work in computed tomography that has shown that the combination of functional and anatomical information can provide results that are superior to either type of data on its own [28].

Coronary MRA – inclusion into FB protocol

In order to take advantage of recently developed rapid FB CAD CMR protocol, we used a coronary MRA prototype WIP sequence[1] developed in collaboration with King's College London that acquires a full coronary 3D dataset within the 5–10 minute window prior to the LGE image acquisition. The sequence uses a 2D image-based navigation (iNAV) [29], a two-point Dixon acquisition with bipolar readout gradients for improved fat suppression [30] and a variable density spiral-like Cartesian (VD-CASPR) trajectory [31, 32] with non-rigid motion-compensated reconstruction [33]. Basic scan parameters on our MAGNETOM Skyra^{fit} scanner included a 3D spoiled gradient echo sequence, FOV 320 x 320 x 90–130 mm for an isotropic spatial resolution of 1.0 mm^3, bandwidth 967 Hz/px, subject specific acquisition window of 70–100 ms, and a 2D iNAV preceding the VD-CASPR acquisition [32]. Undersampling between 5x and 10x was chosen to maintain an acquisition time of around 5–8 minutes, depending on the patient's heart rate. A predictable scan time and 100% respiratory scan efficiency is achieved using a non-rigid motion-compensated iterative reconstruction that is performed in-line on the MARS computer. An example of the sequence setup is shown in Figure 2. The radiographer has to determine the extent of the transversal slab in the coronal plane to include the whole heart, and position the iNAV window within the left ventricle and two saturation bands to cover the arms. Minimum preparation is required for the acquisition beyond these steps. The sequence then outputs four image datasets (Fig. 3): an in-phase, an out-of-phase, a water, and a fat volume.

In order to choose a quiet cardiac phase to acquire the CMRA, we use another prototype[1] for AI-based resting phase detection on a 4-chamber FB CINE prior to the coronary acquisition. The AI algorithm is able to detect and track the motion of the right coronary artery (RCA) located at the atrio-ventricular junction in that cine image [34]. The sequence then generates a graphic motion curve of the RCA throughout the cycle, automatically detecting the best resting phase(s). The time and length of the scan window can be manually edited by adjusting the trigger delay visually, making it a highly customizable option if one chooses to use a systolic or diastolic phase, for example. In Figure 4, an example of the RCA tracking at diastole and systole plus the motion curve and detected resting phases as displayed in the 3D protocol is shown.

Given the ability to perform sequence setup and acquisition in less than 10 minutes, we routinely included this sequence in all our protocols where the information regarding coronary anatomy would be clinically valuable, using the interval prior to LGE imaging in order to avoid extending the exam unnecessarily (Fig. 1B).

[1] *Work in progress: the application is currently under development and is not for sale in the U.S. and in other countries. Its future availability cannot be ensured.*

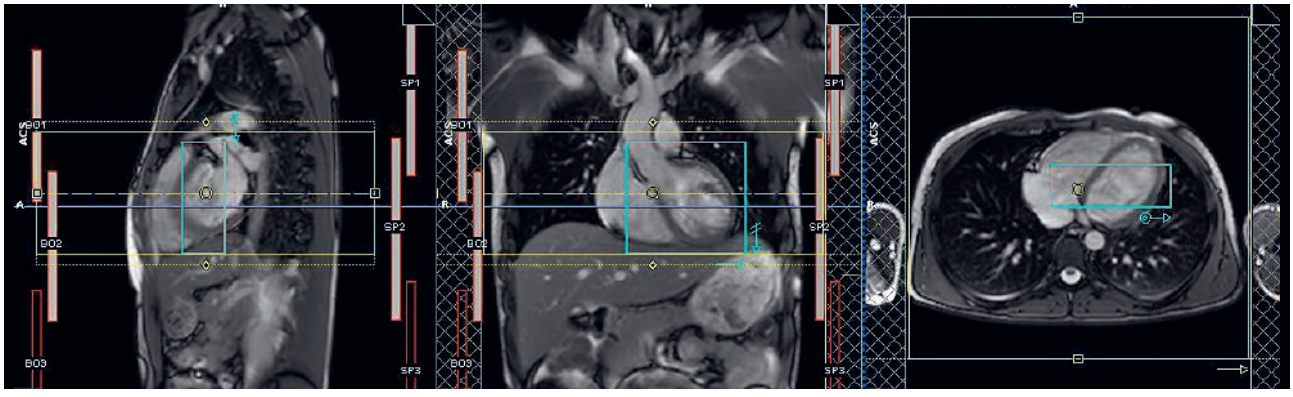

2 A typical whole-heart 3D coronary magnetic resonance angiography (MRA) setup; in yellow, the field of view can be seen with saturation slabs on the arms for signal suppression; at 3T and using the Cartesian spoiled gradient echo acquisition, no specific shim box needs to be established, with coverage of the whole slab; in blue, the 2D image-based navigation (iNAV) tracking in both read and phase directions over the left ventricle.

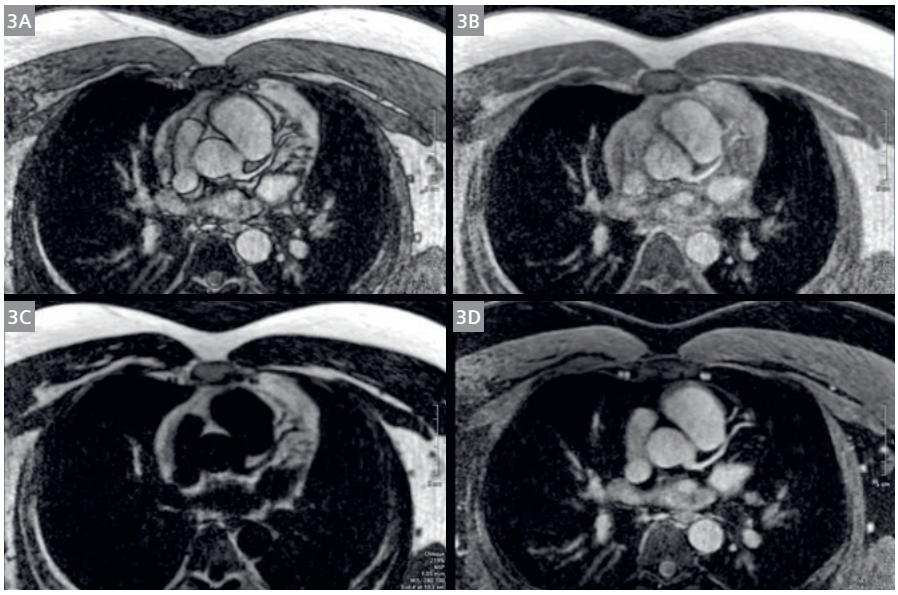

3 The output from the 3D whole-heart coronary magnetic resonance angiography (MRA) sequence used in this study:
(3A) out-of-phase images;
(3B) in-phase images;
(3C) fat-reconstructed images;
(3D) water-reconstructed images.
Most of the time, reading of the coronary MRA was performed only with the water-reconstructed dataset, although the other images may also be used to check for potential artifacts or other anatomical areas of interest outside the coronary tree.

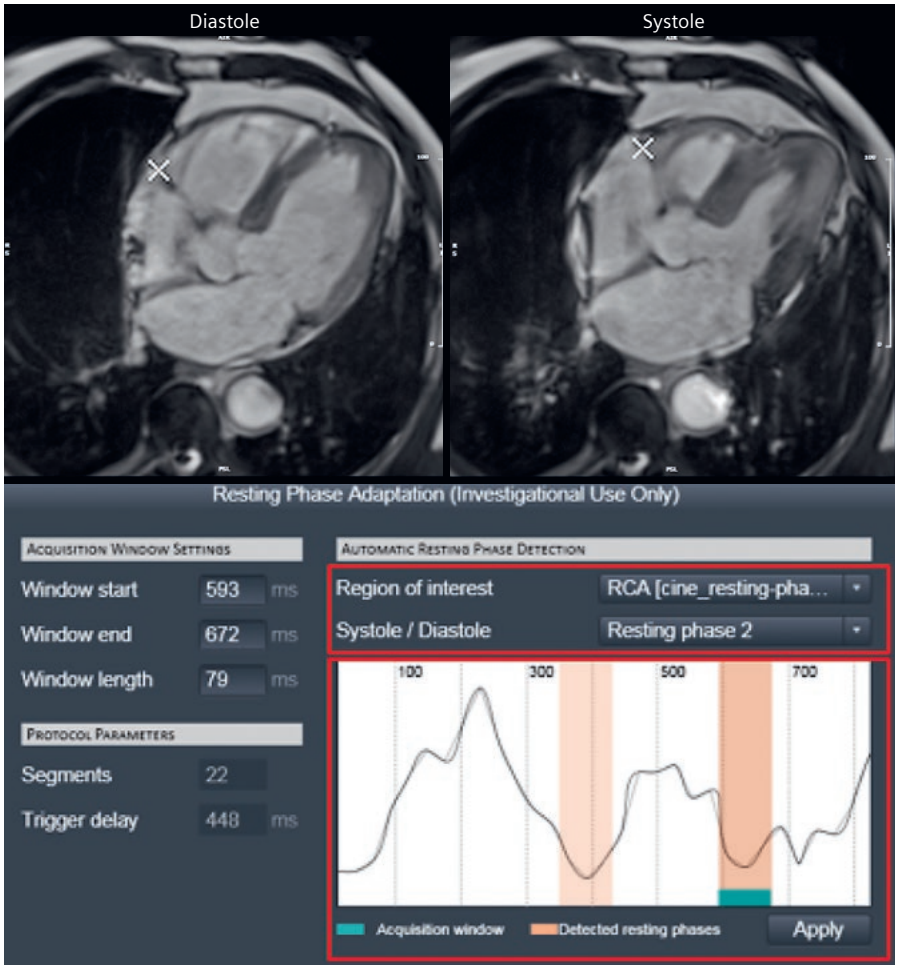

4 The AI-based resting phase detection for static cardiac imaging output is shown after acquiring a free-breathing cine in the 4-chamber long-axis view. The algorithm detects the right coronary artery location and tracks its movement during the cardiac phase (identified in X). It then generates a curve graph depicting the movement and automatically suggests the optimal phase and window length for the best resting phase(s) of the coronary images. This can be manually edited and the user can configure whether to image in systole or diastole, and can set the temporal resolution of the acquisition. Shorter window lengths increase the exam time but shortens the scan-window within one heart-beat, while longer window lengths decrease the total exam time.

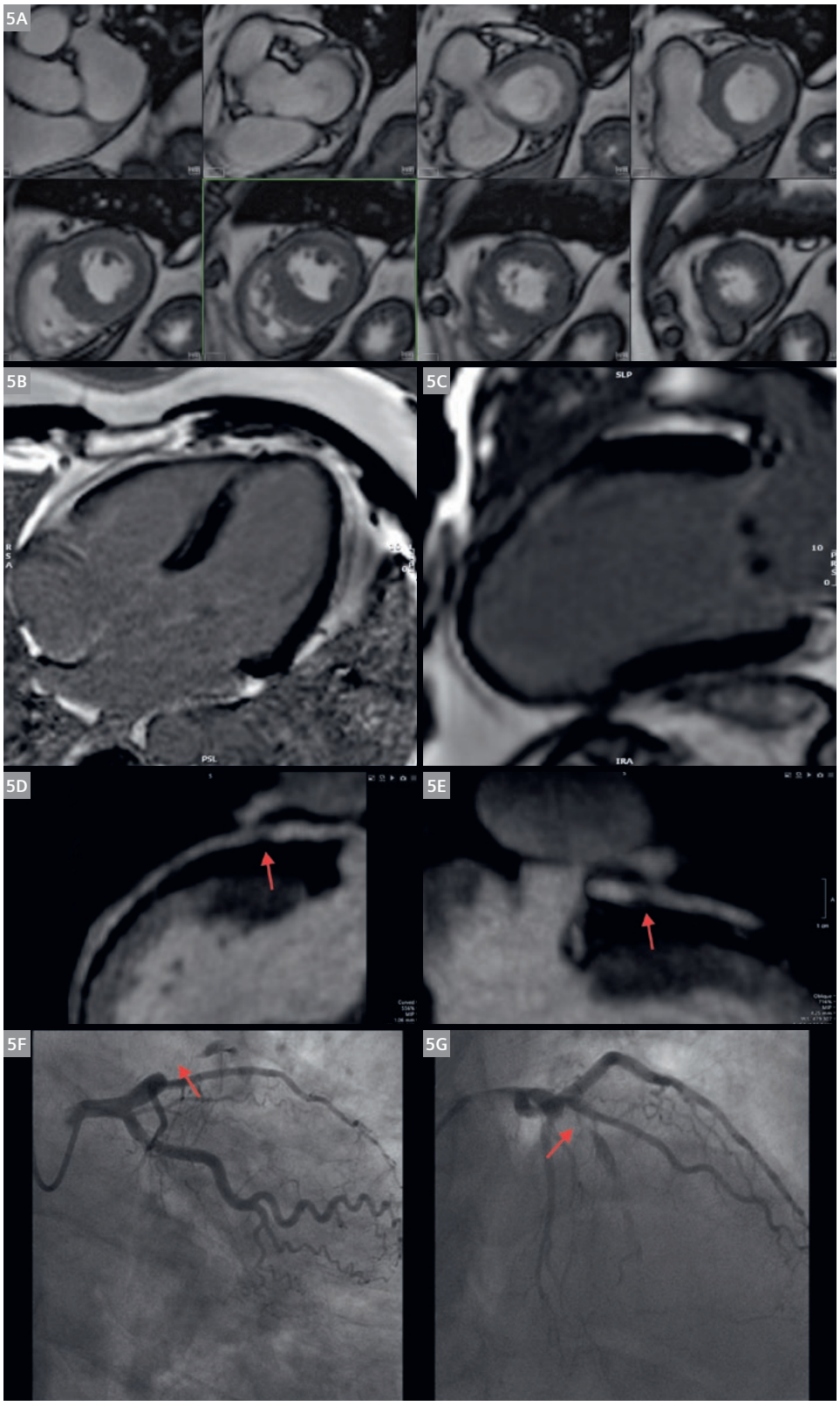

5 **(5A)** In the systolic frame of a short-axis binning FB cine, where one can identify the antero-septal mid-apical segmental hypocontractility; **(5B and C)** show late gadolinium enhanced (LGE) images with a subendocardial infarct in the same segments; **(5D and E)** the left anterior descending (LAD) artery shows a severe obstructive lesion identified in the proximal segment of the artery (red arrows); **(5F and G)** reveal the subsequent invasive angiogram that identified an occluded proximal LAD (red arrows), confirming the findings from the coronary magnetic resonance angiography MRA.

Clinical uses of the integrated FB CMR exam

Since the integration of the Whole-Heart CMRA WIP[1] in our protocol in May 2020, we were able to scan over 350 patients using the integrated FB protocol in a heterogeneous population comprising CAD evaluation, cardiomyopathies, arrythmia investigation, and myocarditis. A more in-depth analysis of the clinical utility, effectiveness, and quality obtained with this protocol is underway, but we believe some examples presented here will help other centers to further explore the possibilities that are opening up with these new techniques.

The first case is a 56-year-old male patient who underwent CMR evaluation for recent onset of typical chest pain associated with a segmental deficit identified on a rest echocardiography. CMR confirmed the akinesia in the antero-septal mid-apical segments of the left ventricle (LV), and LGE revealed a subendocardial infarct in areas with viable myocardium (Fig. 5). Coronary MRA suggested a significant lesion in the proximal segment of the left anterior descending artery (LAD) with preserved distal segments of the artery. After the exam, the patient underwent an invasive angiography that confirmed an occluded proximal LAD, that was treated percutaneously.

The second example is a 77-year-old woman who presented with recent shortness of breath, and had a normal exercise ECG test and global LV function by echocardiography. She underwent a CMR exam for further evaluation of her symptoms and to rule out CAD (Fig. 6). Her stress first-pass perfusion exam showed a mild defect in the infero-septal wall throughout the whole extension of the LV, although there was some doubt regarding whether the finding represented a true defect. LGE images demonstrated an inferior infarct in the apical segment, comprising 50–75% of the area of that segment. The complementary coronary MRA revealed a dominant left circumflex artery with a significant proximal lesion. The LAD artery was normal (not shown). Coronary MRA confirmed that the perfusion defect was indeed a true defect, and the patient subsequently underwent invasive angiography that confirmed the CMR findings, and was treated accordingly.

The third example is a 32-year-old man, for whom a CMR was requested to investigate the hypothesis of myocarditis after episodes of chest pain and raised serum troponin. His initial native T1 values in a long-axis view (Fig. 7) were normal in the septal region but decreased in the basal portion of the infero-lateral wall (1232 ms and 1057 ms respectively, at 3T). LGE images did not reveal a pattern typical of myocarditis, but they did show a transmural lesion with a dark center compatible with a recent infarct with areas of no-reflow. The coronary MRA images obtained further supported these results, better depicting the area of no-reflow shown in the LGE images. Coronary evaluation revealed a normal right coronary artery (RCA) and LAD, and a significant lesion in the mid portion of the circumflex artery just after the take-off of the first left marginal branch. CMR findings excluded the hypothesis of myocarditis and the patient was treated accordingly.

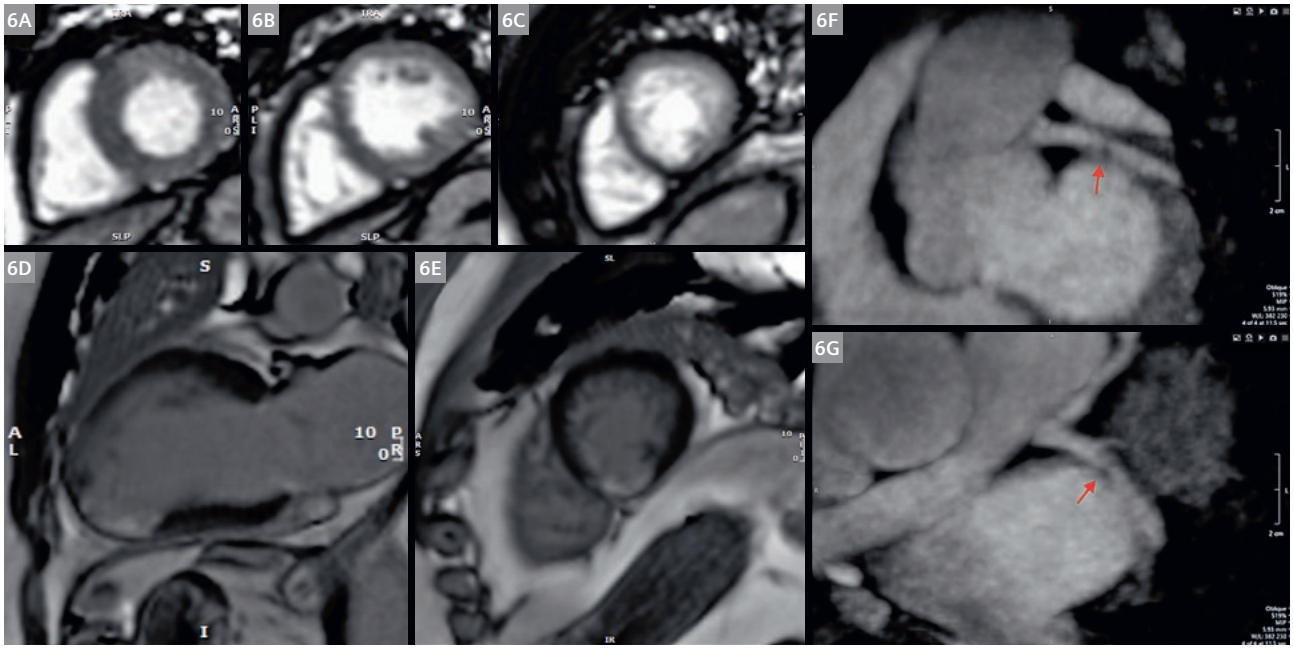

6 First-pass stress perfusion images of the basal **(6A)**, mid **(6B)**, and apical **(6C)** segments suggested reduced perfusion in the infero-septal wall along the full extension of the left ventricle, but some questions were raised about whether the defect represented true perfusion defects; **(6D and E)** corresponding LGE images that identified an inferior apical infarct; **(6F and G)** show the coronary MRA images of the dominant left circumflex artery with a significant proximal obstruction corroborating the findings from both the perfusion and LGE images.

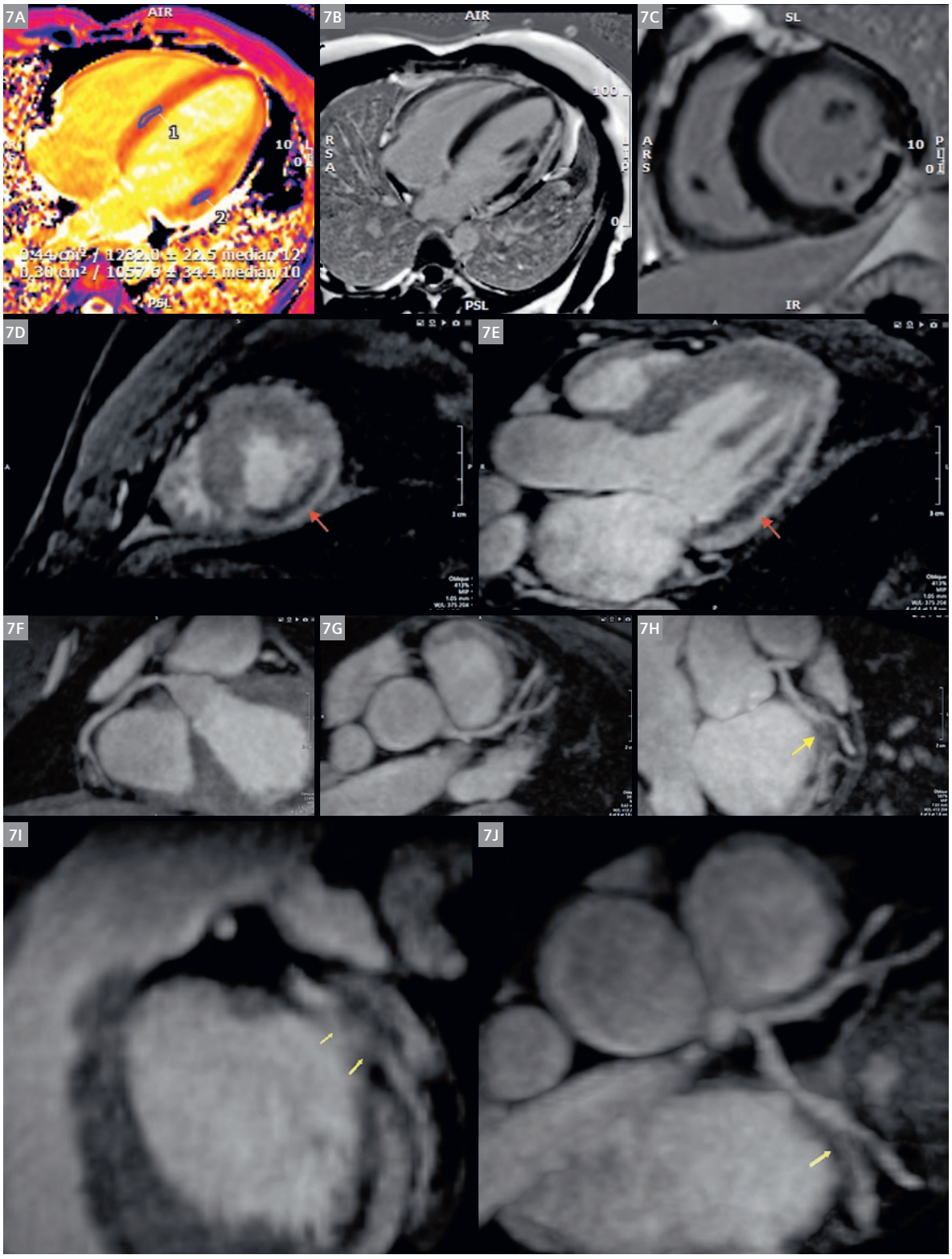

7 In a patient studied to rule out myocarditis, native T1 images **(7A)** identified a lower T1 value in the lateral wall of the basal segment of the left ventricle (10577 ms at 3T); **(7B and C)** LGE images showing an area of transmural scar in the infero-lateral wall of the left ventricle with a dark center corresponding to an area of no-reflow; **(7D and E)** better identified of the region of no-reflow using the water-reconstructed image from the coronary MRA dataset (red arrows); the right coronary artery **(7F)** and left anterior descending artery **(7G)** were normal; the left circumflex artery **(7H–J)** was occluded in its mid-segment after the take-off of the first marginal branch (yellow arrows).

The final example is shown in Figure 8: a 70-year-old woman who underwent CMR for suspected CAD due to diffusely inverted T waves in her resting ECG and an apparently normal echocardiography. In the cine images, we already observed apical hypertrophy that was probably missed by echo. Quantitative stress perfusion revealed reduced absolute perfusion in the subendocardial portion of the apical segments, co-localized with the hypertrophic regions seen in the cine images. LGE did not demonstrate any fibrosis. The coronary MRA images showed normal coronary arteries, confirming that the perfusion defects observed were due to microcirculatory deficits common in hypertrophic cardiomyopathies, and not a result of epicardial obstruction of the coronary arteries. The patient then underwent a coronary CTA, which confirmed the findings from the coronary MRA.

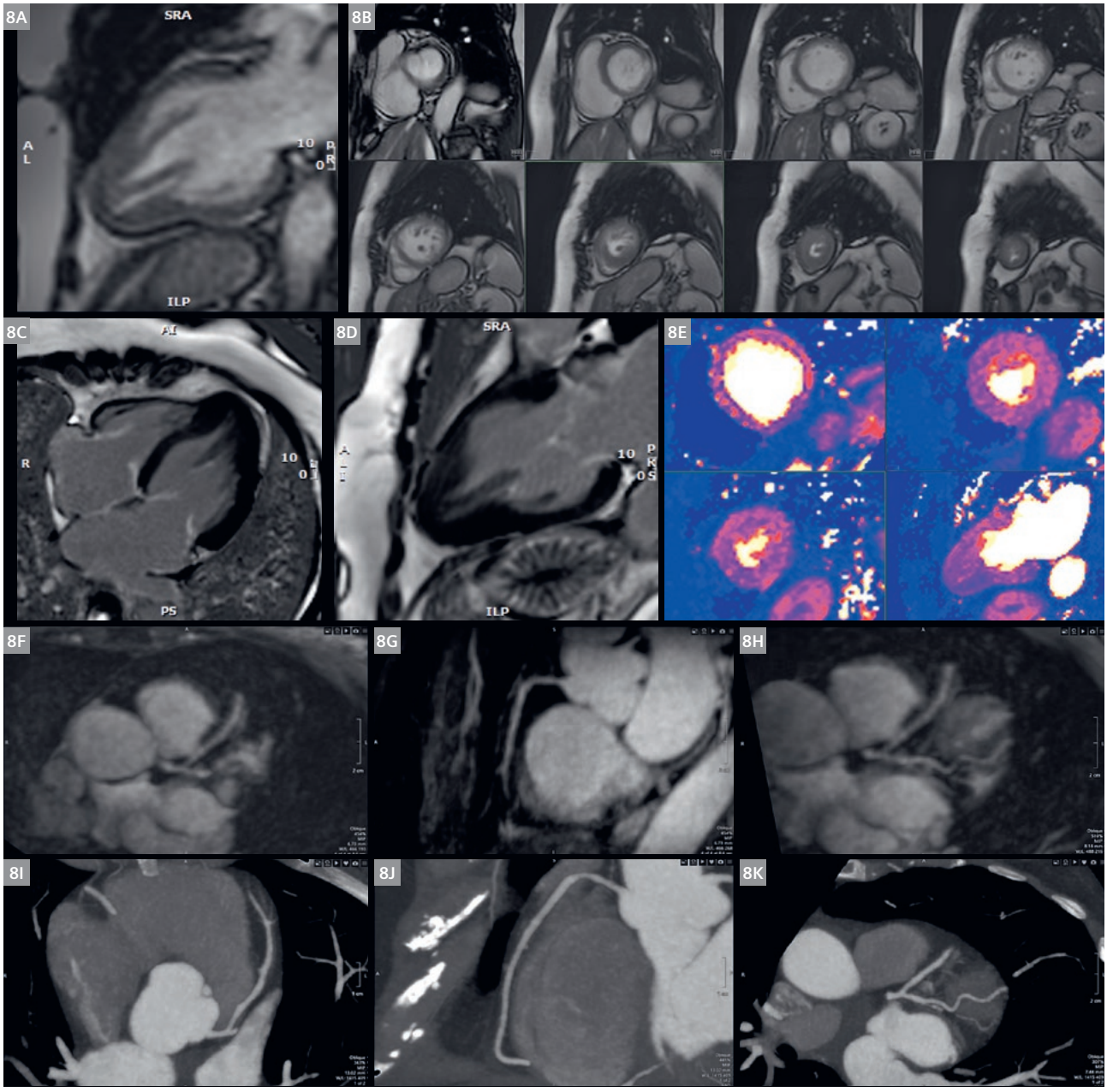

8 Cine images **(8A and B)** illustrate the apical hypertrophy of the left ventricle in a 2-chamber and short-axis view; **(8C and D)** long-axis LGE images confirm the hypertrophy but did not identify any associated scars in those segments; **(8E)** quantitative first-pass stress perfusion shows mild reduction in myocardial blood flow in the subendocardial areas of the hypertrophic segments, but the coronary MRA images of the left anterior descending artery **(8F)**, right coronary artery **(8G)**, and left circumflex **(8H)** did not identify any significant lesions, attributing the perfusion findings to microcirculatory impairment found in the primary cardiomyopathy; **(8I–K)** the patient underwent a further coronary computed tomography angiography (CTA) that confirmed the coronary MRA findings.

Standalone coronary MRA exams

Apart from integrating the coronary MRA with other routine CMR sequences, we also explored the possibility of using the sequence as a standalone exam for coronary MRA anatomical evaluation per se. Our center performs a high number of coronary CTAs and it is not uncommon to find patients who have that exam ordered, but either do not consent to receiving contrast or have a significant contraindication to the exam (a history of severe allergic reactions or high-risk kidney disease, for example). In cases where the pre-test likelihood for CAD was low but the CTA exam was requested anyway, we believe that coronary MRA can be of value, especially in young patients[2], even when performed alone and without the other information gathered in a routine CMR exam.

The protocol used in our center for these cases was to initially perform a non-contrast CT exam for calcium score in patients with the aforementioned history. If the calcium score was zero, revealing a very low probability of obstructive coronary disease given the already low pre-test clinical probability, the patient would undergo a coronary MRA without the use of contrast. We have performed 17 of these cases since the installation of the sequence, and no coronary CTA with contrast was subsequently requested in any of them, suggesting that this can be a valid alternative in this setting, providing further evidence.

In these cases, the objective of the coronary MRA is to rule out obstructive CAD in patients with low probability of the disease. The CMR protocol requires only localizers and use of the AI-based resting phase detection based on FB 4-chamber CINE followed by the whole-heart MRA. As this is a dedicated exam with more time available in the scanner, we perform two separate acquisitions in both systole and diastole, in order to improve the accuracy of the exam and eliminate artifacts that may be caused by coronary motion in either cardiac phase. Figure 9 shows the example of a 38-year-old woman who had suffered a severe allergic reaction to iodinated contrast prior to her coronary CTA request. She first underwent a non-contrast CT exam, which showed a calcium score of zero. She then underwent a coronary MRA with images obtained both in systole and diastole, ruling out significant obstructive CAD.

Limitations and future developments

The current WIP sequences[1] used in the last six months allowed us to perform coronary MRAs in a busy clinical routine without significant impact on examination time. We believe that, coupled with the use of a full FB CMR protocol and quantitative perfusion analysis, the anatomical and functional data provided by this comprehensive exam can be very competitive in providing the most useful clinical information in a relatively short exam time and with no radiation, singling out CMR as the only imaging modality that can offer this possibility. The current implementation of the whole-heart coronary MRA technique allows the sequence to become truly usable in clinical routine. While the current spatial resolution is not yet matching that of coronary CTA technology, the CMR alternative is a genuine option for ruling out coronary disease, as we have experienced in these initial cases.

A few challenges still remain, and we list them here so that other centers can collaborate in further developing what is now a very mature option for anatomical coronary assessment. First, in all the exams we performed, no particular attention was given to optimizing the coronary exam using either nitrates or beta-blockers. The goal was to test-drive the sequence in a real clinical environment and under any possible circumstances, including cases involving arrhythmias, obesity, tachycardia, etc. While the benefits of both drugs in coronary CTA are well known, the experience in CMR is very limited [35]. Exploring the possible benefits of using these drugs for coronary MRA is necessary for accurately comparing the findings of this technique with coronary CTA. The second question regards the influence of contrast agents on SNR. In our cases, most patients were studied after having received contrast so possibly the current SNR/CNR observed is influenced by the protocol design. Having said that, in the cases of isolated coronary MRAs, no contrast was used and we did not observe a significant change in signal compared to the contrast enhanced exams (visual observation). But, again, this is another issue that merits further investigation as it has an important impact on the workflow.

Another possible use of these sequences is in children[2], since it can prevent any use of ionizing radiation and contrast injection. Given that most coronary evaluations in children are not intended to assess atherosclerotic obstructions, which require higher spatial resolution, this particular coronary sequence can be very useful as it provides a full FB acquisition with 100% respiratory efficacy and predictable scan time. Finally, the current implementation of whole-heart coronary MRA still cannot help us answer questions concerning patients with stents or bypass grafts, as most of these cases involve metal artifacts. What is more, we also observed some lower image quality when assessing the distal segments of the RCA, especially the posterior descending artery branch and posterior ventricular artery branch. Finally, atherosclerotic evaluation and the determination of coronary plaques are emerging as key elements for establishing the patient's prognosis and guiding clinical treatment. Current CMRA sequences only provide limited information with regard to coronary plaque. This is one of the reasons why we opted

[2]MR scanning has not been established as safe for imaging fetuses and infants less than two years of age. The responsible physician must evaluate the benefits of the MR examination compared to those of other imaging procedures.

to add a CT calcium score in patients that underwent a standalone anatomical coronary study. Reducing the current spatial resolution to something closer to 0.5 mm^3 is still desirable as long as acquisition time can still be kept below 10 minutes.

Conclusions

In conclusion, our current experience with integrating coronary anatomical information into a full FB CMR protocol has been very positive, adding very little overhead in terms of exam time while providing us with new information to support our clinical diagnosis and therapeutic decisions. The current 3D whole-heart sequences could be incorporated in a busy clinical service and also provided an alternative imaging option to patients who did not consent or had a contraindication to an iodinated contrast exam. However, there are many questions that remain despite this initial experience. We encourage other centers to engage in this development, as the impact of coronary anatomical evaluation in clinical practice is rapidly being revisited with the growing use of CTA. CMR has potential for incorporating that information in addition to all the unique functional data that it already provides, especially if more centers contribute to the advancement of this technique.

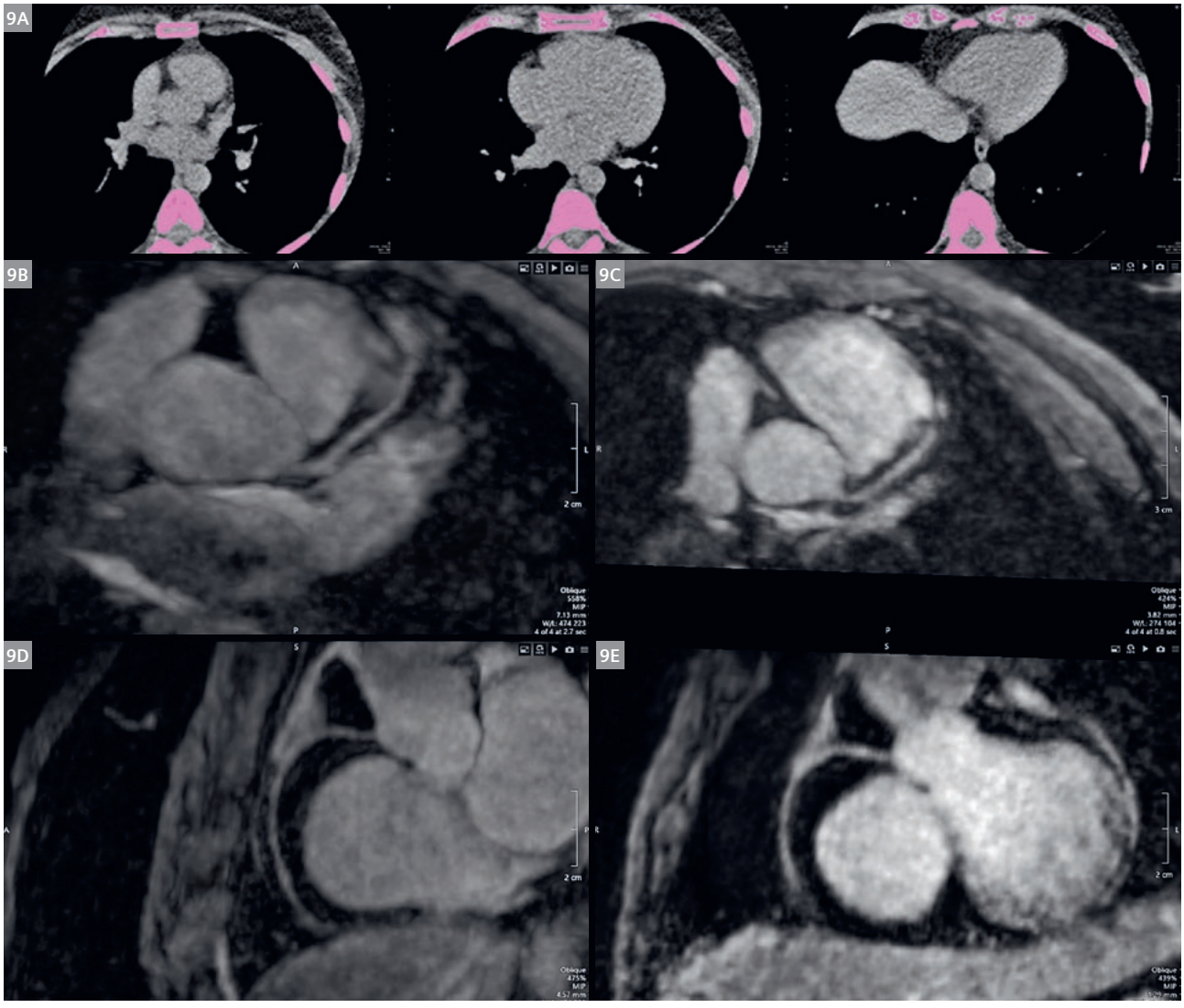

9 A patient with contra-indications for a contrast coronary CTA underwent a non-contrast calcium score exam with a score of zero **(9A, part of the dataset)**; she then underwent a non-contrast coronary MRA that revealed normal coronary arteries with no significant obstructions, ruling out significant coronary artery disease; **(9B and D)** the left anterior descending artery and right coronary artery were imaged during diastole; **(9C and E)** the same arteries imaged during systole; both datasets were obtained in order to increase the accuracy of the interpretation and rule out potential artifacts; this strategy is also used when reading coronary CTAs, especially when patients are arrhythmic and an increased acquisition window is used.

Acknowledgments

The Siemens Healthineers Whole-Heart team for development and setup of the free-breathing whole-heart CMRA sequence.

Peter Kellman and Hui Xue (Medical Signal and Image Processing Program at the NHLBI, USA) for setting up and providing the cine, LGE, and quantitative perfusion FB sequences used in the protocols described within the Gadgetron framework.

References

1 Kwong RY, Ge Y, Steel K, Bingham S, Abdullah S, Fujikura K, Wang W, Pandya A, Chen YY, Mikolich JR, Boland S, Arai AE, Bandettini WP, Shanbhag SM, Patel AR, Narang A, Farzaneh-Far A, Romer B, Heitner JF, Ho JY, Singh J, Shenoy C, Hughes A, Leung SW, Marji M, Gonzalez JA, Mehta S, Shah DJ, Debs D, Raman SV, Guha A, Ferrari VA, Schulz-Menger J, Hachamovitch R, Stuber M, Simonetti OP. Cardiac Magnetic Resonance Stress Perfusion Imaging for Evaluation of Patients With Chest Pain. J Am Coll Cardiol. 2019;74:1741-1755.

2 Nagel E, Greenwood JP, McCann GP, Bettencourt N, Shah AM, Hussain ST, Perera D, Plein S, Bucciarelli-Ducci C, Paul M, Westwood MA, Marber M, Richter WS, Puntmann VO, Schwenke C, Schulz-Menger J, Das R, Wong J, Hausenloy DJ, Steen H, Berry C, Investigators M-I. Magnetic Resonance Perfusion or Fractional Flow Reserve in Coronary Disease. N Engl J Med. 2019;380:2418-2428.

3 Ullah W, Roomi S, Abdullah HM, Mukhtar M, Ali Z, Ye P, Haas DC, Figueredo VM. Diagnostic Accuracy of Cardiac Magnetic Resonance Versus Fractional Flow Reserve: A Systematic Review and Meta-Analysis. Cardiol Res. 2020;11:145-154.

4 Greenwood JP, Ripley DP, Berry C, McCann GP, Plein S, Bucciarelli-Ducci C, Dall'Armellina E, Prasad A, Bijsterveld P, Foley JR, Mangion K, Sculpher M, Walker S, Everett CC, Cairns DA, Sharples LD, Brown JM, Investigators C-M. Effect of Care Guided by Cardiovascular Magnetic Resonance, Myocardial Perfusion Scintigraphy, or NICE Guidelines on Subsequent Unnecessary Angiography Rates: The CE-MARC 2 Randomized Clinical Trial. JAMA. 2016;316:1051-60.

5 Knott KD, Fernandes JL, Moon JC. Automated Quantitative Stress Perfusion in a Clinical Routine. Magn Reson Imaging Clin N Am. 2019;27:507-520.

6 Maron DJ, Hochman JS, Reynolds HR, Bangalore S, O'Brien SM, Boden WE, Chaitman BR, Senior R, Lopez-Sendon J, Alexander KP, Lopes RD, Shaw LJ, Berger JS, Newman JD, Sidhu MS, Goodman SG, Ruzyllo W, Gosselin G, Maggioni AP, White HD, Bhargava B, Min JK, Mancini GBJ, Berman DS, Picard MH, Kwong RY, Ali ZA, Mark DB, Spertus JA, Krishnan MN, Elghamaz A, Moorthy N, Hueb WA, Demkow M, Mavromatis K, Bockeria O, Peteiro J, Miller TD, Szwed H, Doerr R, Keltai M, Selvanayagam JB, Steg PG, Held C, Kohsaka S, Mavromichalis S, Kirby R, Jeffries NO, Harrell FE, Jr., Rockhold FW, Broderick S, Ferguson TB, Jr., Williams DO, Harrington RA, Stone GW, Rosenberg Y, Group IR. Initial Invasive or Conservative Strategy for Stable Coronary Disease. N Engl J Med. 2020;382:1395-1407.

7 Saraste A, Barbato E, Capodanno D, Edvardsen T, Prescott E, Achenbach S, Bax JJ, Wijns W, Knuuti J. Imaging in ESC clinical guidelines: chronic coronary syndromes. Eur Heart J Cardiovasc Imaging. 2019;20:1187-1197.

8 Knuuti J, Wijns W, Saraste A, Capodanno D, Barbato E, Funck-Brentano C, Prescott E, Storey RF, Deaton C, Cuisset T, Agewall S, Dickstein K, Edvardsen T, Escaned J, Gersh BJ, Svitil P, Gilard M, Hasdai D, Hatala R, Mahfoud F, Masip J, Muneretto C, Valgimigli M, Achenbach S, Bax JJ, Group ESCSD. 2019 ESC Guidelines for the diagnosis and management of chronic coronary syndromes. Eur Heart J. 2020;41:407-477.

9 Ge Y, Pandya A, Steel K, Bingham S, Jerosch-Herold M, Chen YY, Mikolich JR, Arai AE, Bandettini WP, Patel AR, Farzaneh-Far A, Heitner JF, Shenoy C, Leung SW, Gonzalez JA, Shah DJ, Raman SV, Ferrari VA, Schulz-Menger J, Hachamovitch R, Stuber M, Simonetti OP, Kwong RY. Cost-Effectiveness Analysis of Stress Cardiovascular Magnetic Resonance Imaging for Stable Chest Pain Syndromes. JACC Cardiovasc Imaging. 2020;13:1505-1517.

10 Kramer CM. Potential for Rapid and Cost-Effective Cardiac Magnetic Resonance in the Developing (and Developed) World. J Am Heart Assoc. 2018;7:e010435.

11 Kim WY, Danias PG, Stuber M, Flamm SD, Plein S, Nagel E, Langerak SE, Weber OM, Pedersen EM, Schmidt M, Botnar RM, Manning WJ. Coronary magnetic resonance angiography for the detection of coronary stenoses. N Engl J Med. 2001;345:1863-9.

12 Kato Y, Ambale-Venkatesh B, Kassai Y, Kasuboski L, Schuijf J, Kapoor K, Caruthers S, Lima JAC. Non-contrast coronary magnetic resonance angiography: current frontiers and future horizons. MAGMA. 2020;33:591-612.

13 Hajhosseiny R, Bustin A, Munoz C, Rashid I, Cruz G, Manning WJ, Prieto C, Botnar RM. Coronary Magnetic Resonance Angiography: Technical Innovations Leading Us to the Promised Land? JACC Cardiovasc Imaging. 2020;13:2653-2672.

14 Fernandes JL, Fioravante LA, Zenge MO, Forman C, Schmidt M, Nadar MS, Mazo PE, Greiser A, Speier P, Staeb D, Xue H, Hansen MS, Kellman P, Strecker R. A Comprehensive Free-Breathing Protocol for Cardiovascular Magnetic Resonance Imaging of Ischemia and Cardiomyopathies: a Feasibility Study. Journal of Cardiovascular Magnetic Resonance. 2016;18:P313.

15 Hansen MS, Sorensen TS. Gadgetron: an open source framework for medical image reconstruction. Magn Reson Med. 2013;69:1768-76.

16 Ledesma-Carbayo MJ, Kellman P, Hsu LY, Arai AE, McVeigh ER. Motion corrected free-breathing delayed-enhancement imaging of myocardial infarction using nonrigid registration. J Magn Reson Imaging. 2007;26:184-90.

17 Kellman P, Hansen MS, Nielles-Vallespin S, Nickander J, Themudo R, Ugander M, Xue H. Myocardial perfusion cardiovascular magnetic resonance: optimized dual sequence and reconstruction for quantification. J Cardiovasc Magn Reson. 2017;19:43.

18 Engblom H, Xue H, Akil S, Carlsson M, Hindorf C, Oddstig J, Hedeer F, Hansen MS, Aletras AH, Kellman P, Arheden H. Fully quantitative cardiovascular magnetic resonance myocardial perfusion ready for clinical use: a comparison between cardiovascular magnetic resonance imaging and positron emission tomography. J Cardiovasc Magn Reson. 2017;19:78.

19 Xue H, Kellman P, Larocca G, Arai AE, Hansen MS. High spatial and temporal resolution retrospective cine cardiovascular magnetic resonance from shortened free breathing real-time acquisitions. J Cardiovasc Magn Reson. 2013;15:102.

20 Xue H, Inati S, Sorensen TS, Kellman P, Hansen MS. Distributed MRI reconstruction using Gadgetron-based cloud computing. Magn Reson Med. 2015;73:1015-25.

21 Cross R, Olivieri L, O'Brien K, Kellman P, Xue H, Hansen M. Improved workflow for quantification of left ventricular volumes and mass using free-breathing motion corrected cine imaging. J Cardiovasc Magn Reson. 2016;18:10.

22 Greenwood JP, Maredia N, Younger JF, Brown JM, Nixon J, Everett CC, Bijsterveld P, Ridgway JP, Radjenovic A, Dickinson CJ, Ball SG, Plein S. Cardiovascular magnetic resonance and single-photon emission computed tomography for diagnosis of coronary heart disease (CE-MARC): a prospective trial. Lancet. 2012;379:453-60.
23 Heer T, Reiter S, Hofling B, Pilz G. Diagnostic performance of non-contrast-enhanced whole-heart magnetic resonance coronary angiography in combination with adenosine stress perfusion cardiac magnetic resonance imaging. Am Heart J. 2013;166:999-1009.
24 Klein C, Gebker R, Kokocinski T, Dreysse S, Schnackenburg B, Fleck E, Nagel E. Combined magnetic resonance coronary artery imaging, myocardial perfusion and late gadolinium enhancement in patients with suspected coronary artery disease. J Cardiovasc Magn Reson. 2008;10:45.
25 Bettencourt N, Ferreira N, Chiribiri A, Schuster A, Sampaio F, Santos L, Melica B, Rodrigues A, Braga P, Teixeira M, Leite-Moreira A, Silva-Cardoso J, Portugal P, Gama V, Nagel E. Additive value of magnetic resonance coronary angiography in a comprehensive cardiac magnetic resonance stress-rest protocol for detection of functionally significant coronary artery disease: a pilot study. Circ Cardiovasc Imaging. 2013;6:730-8.

Contact

Juliano Lara Fernandes, M.D., Ph.D., M.B.A.
Cardiovascular Department
Radiologia Clinica de Campinas
Jose Michel Kalaf Research Institute
Av Jose de Souza Campos 840
Campinas, SP, Brazil 13092-123
jlaraf@terra.com.br

26 Hamdan A, Doltra A, Huppertz A, Wellnhofer E, Fleck E, Kelle S. Comparison of coronary magnetic resonance and computed tomography angiography for prediction of cardiovascular events. JACC Cardiovasc Imaging. 2014;7:1063-5.
27 Zhang L, Song X, Dong L, Li J, Dou R, Fan Z, An J, Li D. Additive value of 3T cardiovascular magnetic resonance coronary angiography for detecting coronary artery disease. J Cardiovasc Magn Reson. 2018;20:29.
28 Celeng C, Leiner T, Maurovich-Horvat P, Merkely B, de Jong P, Dankbaar JW, van Es HW, Ghoshhajra BB, Hoffmann U, Takx RAP. Anatomical and Functional Computed Tomography for Diagnosing Hemodynamically Significant Coronary Artery Disease: A Meta-Analysis. JACC Cardiovasc Imaging. 2019;12:1316-1325.
29 Henningsson M, Koken P, Stehning C, Razavi R, Prieto C, Botnar RM. Whole-heart coronary MR angiography with 2D self-navigated image reconstruction. Magn Reson Med. 2012;67:437-45.
30 Munoz C, Cruz G, Neji R, Botnar RM, Prieto C. Motion corrected water/fat whole-heart coronary MR angiography with 100% respiratory efficiency. Magn Reson Med. 2019;82:732-742.
31 Bustin A, Ginami G, Cruz G, Correia T, Ismail TF, Rashid I, Neji R, Botnar RM, Prieto C. Five-minute whole-heart coronary MRA with sub-millimeter isotropic resolution, 100% respiratory scan efficiency, and 3D-PROST reconstruction. Magn Reson Med. 2019;81:102-115.
32 Prieto C, Doneva M, Usman M, Henningsson M, Greil G, Schaeffter T, Botnar RM. Highly efficient respiratory motion compensated free-breathing coronary MRA using golden-step Cartesian acquisition. J Magn Reson Imaging. 2015;41:738-46.
33 Cruz G, Atkinson D, Henningsson M, Botnar RM, Prieto C. Highly efficient nonrigid motion-corrected 3D whole-heart coronary vessel wall imaging. Magn Reson Med. 2017;77:1894-1908.
34 Yoon SS, Hoppe E, Schmidt M, Forman C, Chitiboi T, Sharma P, Tillmanns C, Maier A, Wetzl JA. Robust Deep-Learning-based Automated Cardiac Resting Phase Detection: Validation in a Prospective Study. Proc Intl Soc Mag Reson Med. 2020;28:2210.
35 Hajhosseiny R, Bustin A, Rashid I, Cruz G, Radhouene N, Kunze K, Ismail TF, Rajani R, Masci PG, Prieto C, Botnar RM. 3D whole heart CMRA using an image-navigator framework – a clinical comparison study with CCTA and diaphragmatic navigators. ISMRM 2020. 2020:Abstract 2142.32